Dipole emission near a planar multilayer stack

Baptiste Auguié

July 4, 2012

Abstract

The `planar` package solves the electromagnetic problem of dipole emission near a planar multilayer stack. It comprises two sets of functions; i) to compute the effective Fresnel reflection coefficient of a multilayer structure; ii) to evaluate the modified dipolar field as an integral over plane waves reflected at the interface.

1 Fresnel coefficients

The functions `recursive.fresnel` and `multilayer` both compute the Fresnel coefficients for a multilayer stack, using two different methods (recursive application of Fresnel coefficients for a layer; and transfer matrix, respectively). `multilayer` is more versatile in that it also returns the fields and enhancement factors. `recursive.fresnel`, on the other hand, is more robust for some calculations involving lossless layers. Both functions are complemented by a faster implementation in `C++`, though the output is not as comprehensive.

1.1 Multilayer optics

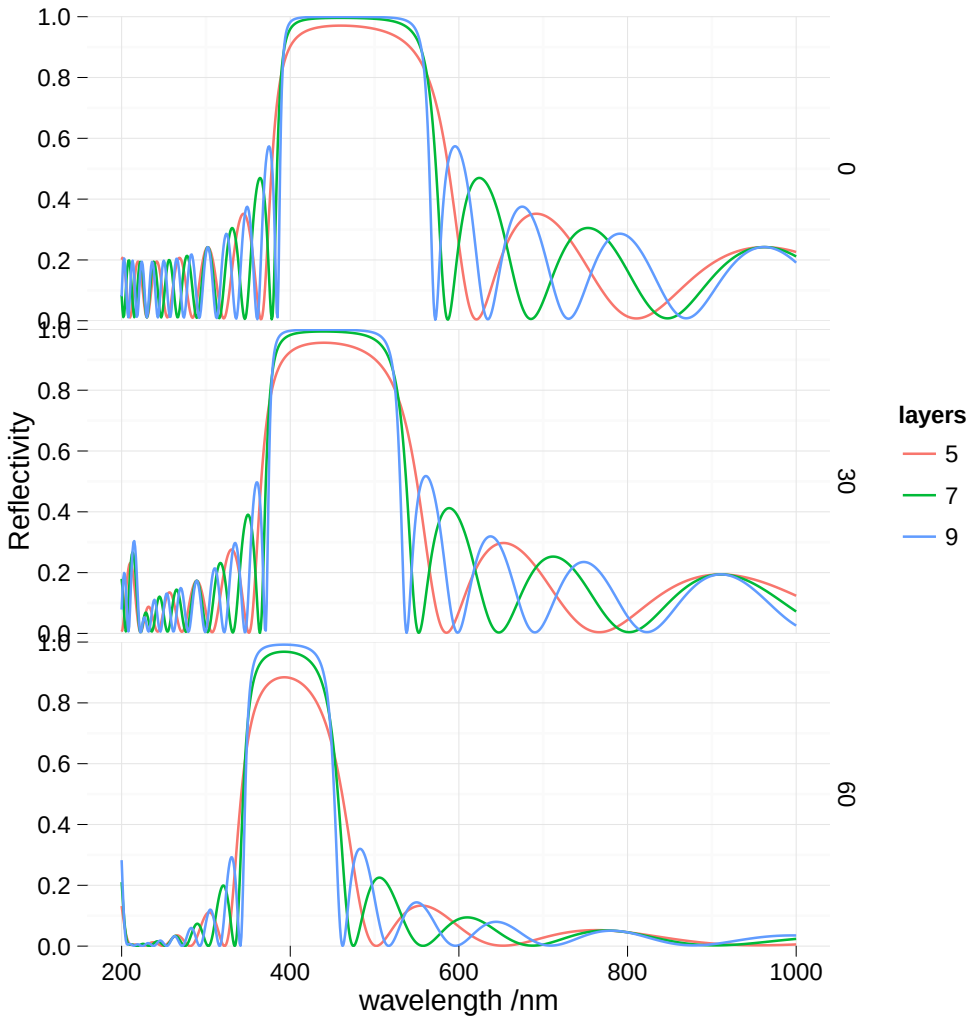

Figure 1: `demo(bragg_stack)`. Reflectivity of a Bragg stack with varying number of layers. Reproducing Fig. 6.6, p. 188 of Mac Leod's Thin Film Optical Filters the structure is a stack of lambda/4 layers of indices nH and nL on a glass substrate with increasing number of layers, the reflectivity stop-band becomes stronger.

1.2 Kretschmann configuration – planar surface plasmon-polaritons

First, we look at the reflectivity of a thin metal film excited in the Kretschmann configuration.

In the same configuration, SPPs may be excited for a wide range of frequencies. The dispersion of the surface mode may be observed as a high

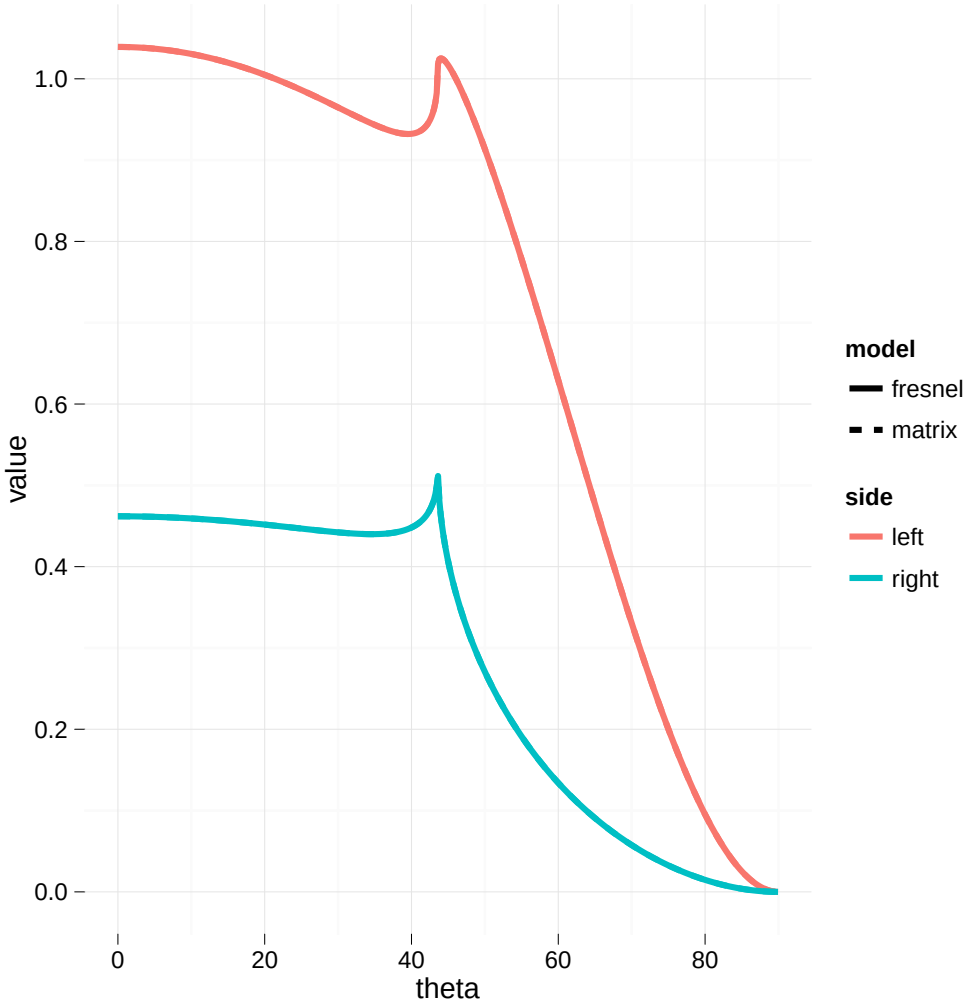

Figure 2: `demo(LFIEF_distance)`. Comparison of the near field enhancement outside of a thin metal film, calculated with i) the transfer matrix method of `multilayer`; ii) Fresnel reflection and transmission coefficients.

reflectivity trace when plotted as a function of incident in-plane wavevector and energy.

Free-space radiation cannot directly couple to SPP modes due to a momentum mismatch. Using evanescent illumination, in-plane wavevectors of arbitrarily large value may be obtained and allow the mapping of the coupled-SPPs dispersion in a symmetric configuration.

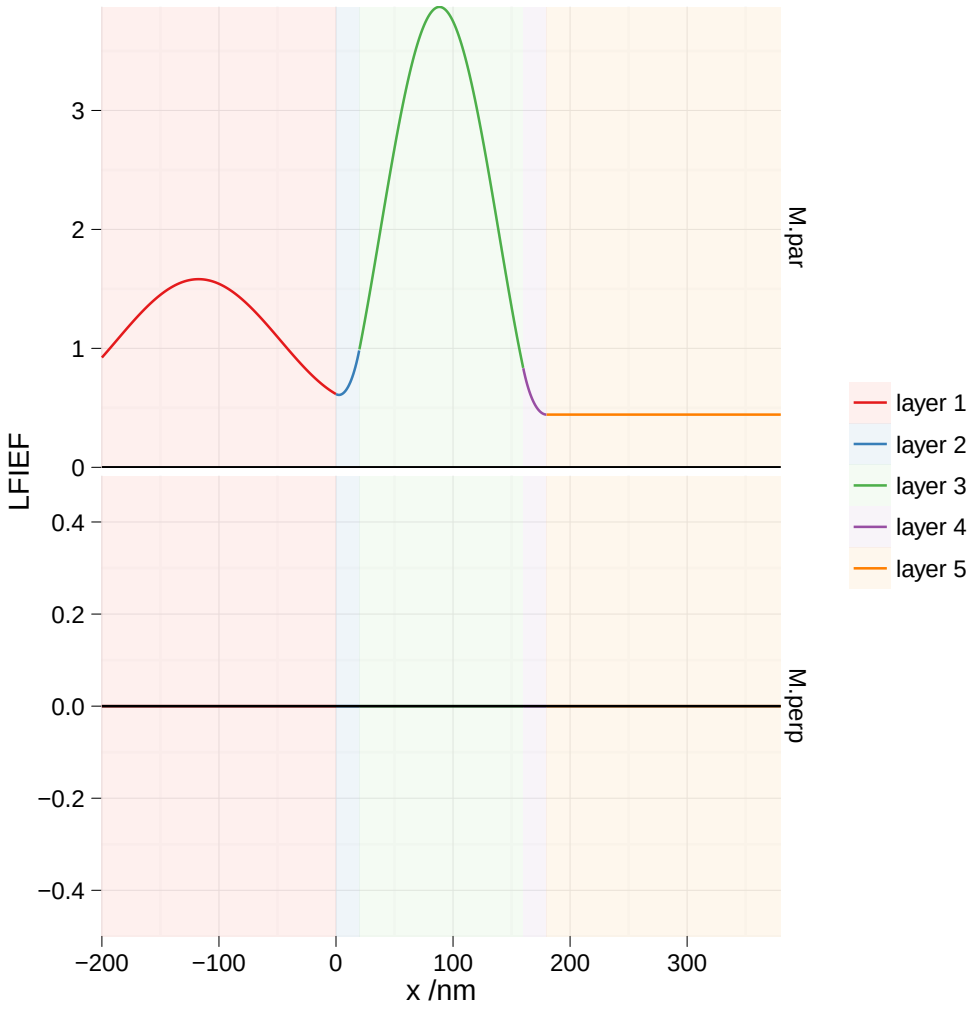

Figure 3: `demo(field_profile_multilayer)`. Local field enhancement factors for a dipole near or inside a multilayer. Note that the field and its derivative are continuous across all interfaces.

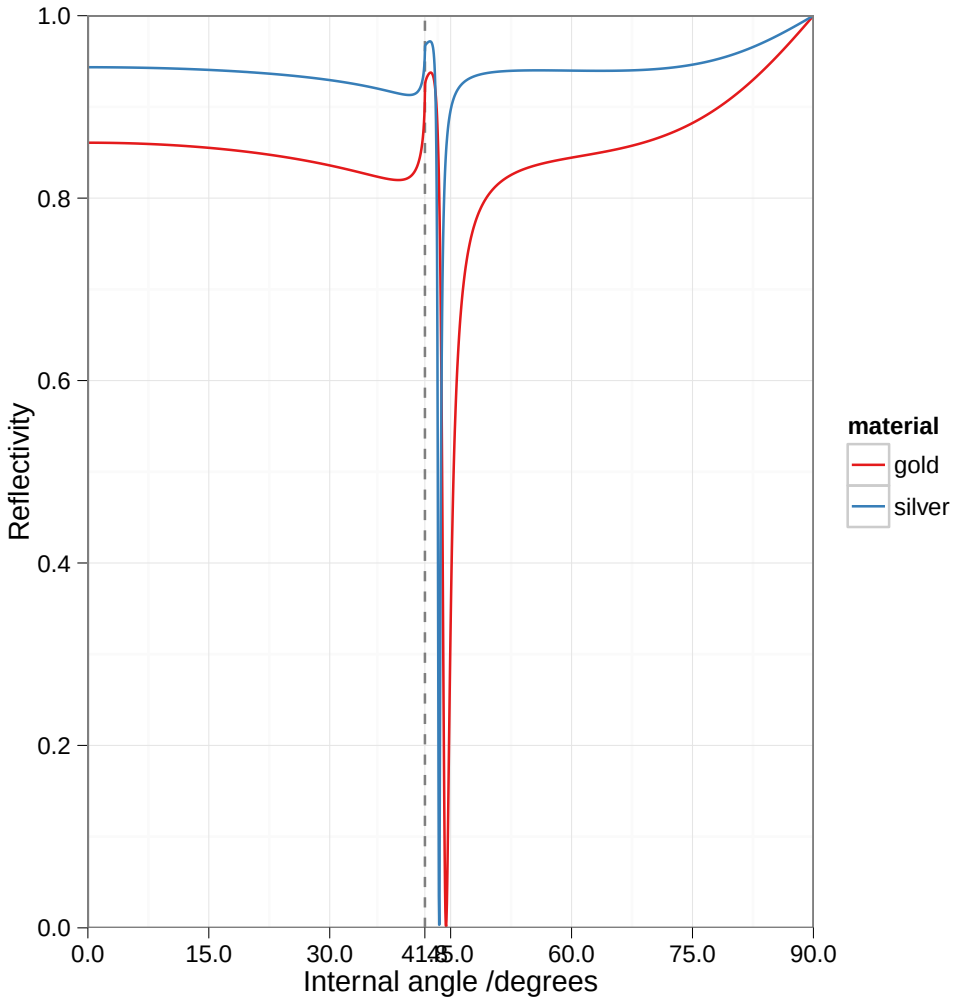

Figure 4: `demo(kretschmann_angle_scan)`. Reflectivity of a thin metal film, 50 nm thick, sandwiched between glass ($n = 1.5$) and air. The SPP is excited at the metal/air interface. By changing the incident angle, the normalised in-plane wavevector q varies from 0 (normal incidence) to 1 (grazing internal angle).

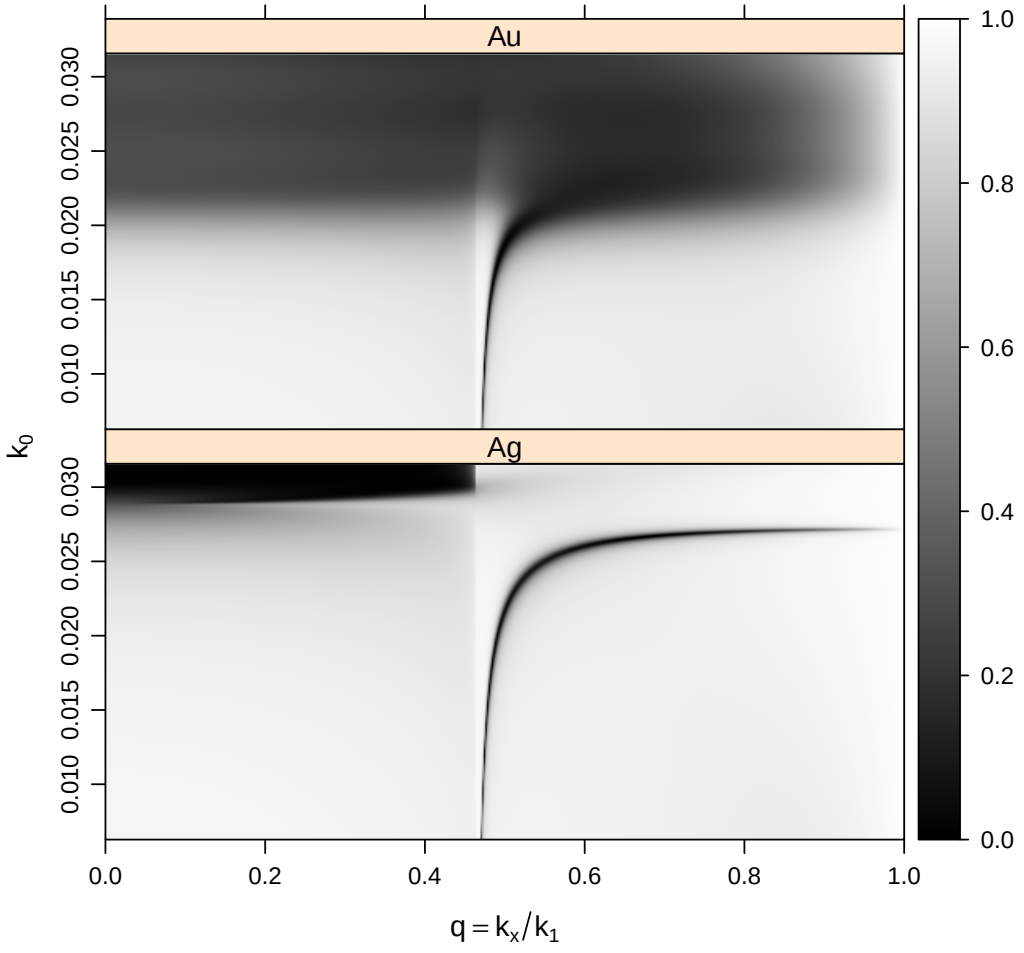

Figure 5: `demo(dispersion_kretschmann)`. Reflectivity of a thin metal film, 50 nm thick, sandwiched between semi-infinite glass ($n = 1.5$) and air. The dispersion of the SPP mode appears as a dark curve following the equation $k_{\mathrm{spp}} = k_0 \sqrt{\frac{\varepsilon_{\mathrm{metal}}\varepsilon_{\mathrm{air}}}{\varepsilon_{\mathrm{metal}}+\varepsilon_{\mathrm{air}}}}$

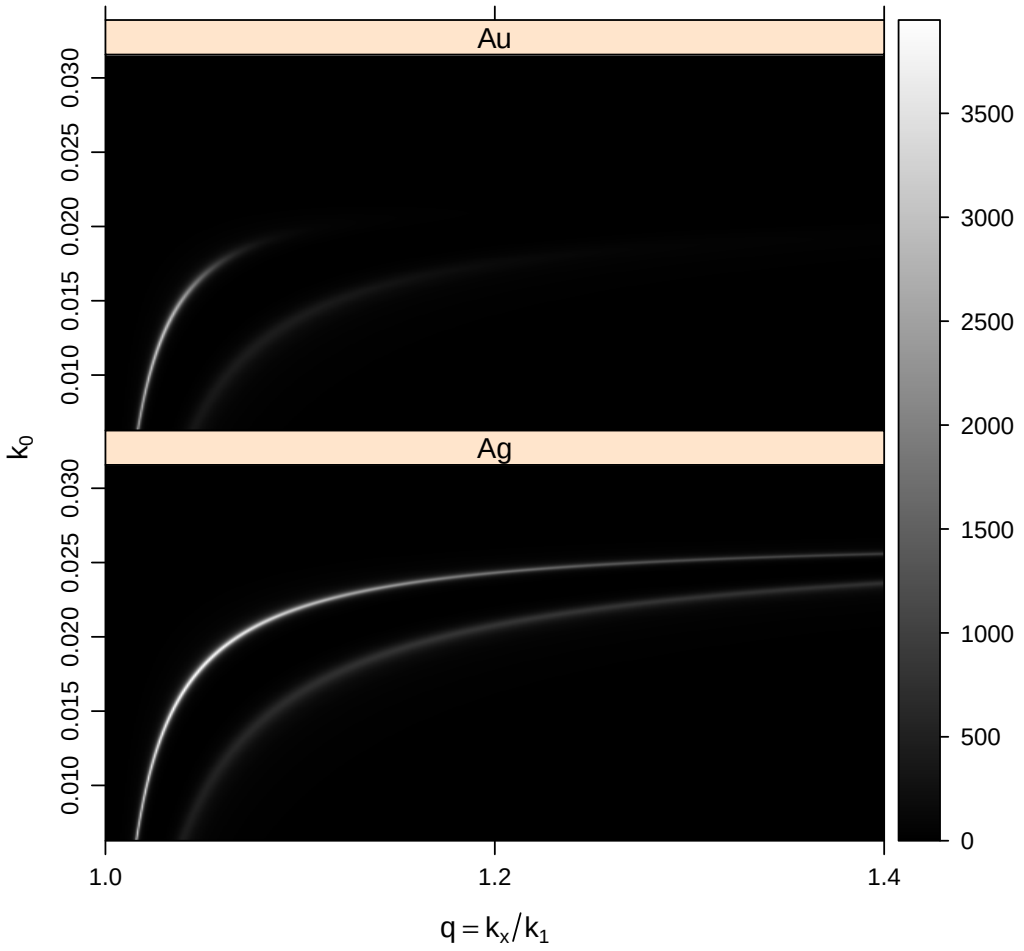

Figure 6: `demo(dispersion_symmetric)`.Reflectivity of a thin metal film, 50 nm thick, sandwiched between semi-infinite glass ($n = 1.5$) on either side. Coupled SPPs are excited when the normalized in-plane wavevector q is greater than 1. Note that values of $|r|^2 > 1$ are not unphysical, as no power is transferred by evanescent waves.

2 Decay rates

From [?] (p. 571), and [?] (pp. 335–360), the total decay rate for a dipole perpendicular to the interface is

$$M_{\text{tot}}^{\perp} = 1 + \frac{3}{2}\int_0^{\infty} \Re\left\{ \frac{q^3}{\sqrt{1-q^2}} r^p(q) \exp\left(2ik_1 d\sqrt{1-q^2}\right)\right\} \mathrm{d}q \tag{1}$$

The integrand diverges as $q \to 1$, it is therefore advantageous to perform the substitution $u := \sqrt{1-q^2}$. In order to maintain a real path of integration, the integral is first split into a radiative region ($0 \le q \le 1$, $u := \sqrt{1-q^2} \ge 0$), and an evanescent region ($1 \le q \le \infty$, $-iu := \sqrt{q^2-1} \ge 0$). After some algebraic manipulation, we obtain,

$$M_{\text{tot}}^{\perp} = 1 + \frac{3}{2}\left(I_1 + I_2\right) \tag{2}$$

where

$$\begin{aligned} I_1 + I_2 = &\int_0^1 \left[1-u^2\right] \cdot \Re\left\{ r^p(\sqrt{1-u^2}) \exp\left(2idk_1 u\right)\right\} \mathrm{d}u \\ &+ \int_0^{\infty} \left[1+u^2\right] \cdot \exp\left(-2dk_1 u\right) \cdot \Im\left\{ r^p(\sqrt{1+u^2})\right\} \mathrm{d}u \end{aligned} \tag{3}$$

Similarly, for the parallel dipole

$$M_{\text{tot}}^{\parallel} = 1 + \frac{3}{4}\int_0^{\infty} \Re\left\{ \left[\frac{r^s(q)}{\sqrt{1-q^2}} - r^p(q)\sqrt{1-q^2}\right] \cdot q \cdot \exp\left(2ik_1 d\sqrt{1-q^2}\right)\right\} \mathrm{d}q \tag{4}$$

which can be rewritten as,

$$M_{\text{tot}}^{\parallel} = 1 + \frac{3}{4}\left(I_1^{\parallel} + I_2^{\parallel}\right) \tag{5}$$

where

$$\begin{aligned} I_1^{\parallel} + I_2^{\parallel} = &\int_0^1 \Re\left\{ \left[r^s(\sqrt{1-u^2}) - u^2 \cdot r^p(\sqrt{1-u^2})\right] \exp\left(2idk_1 u\right)\right\} \mathrm{d}u \\ &+ \int_0^{\infty} \exp\left(-2dk_1 u\right) \cdot \Im\left\{ r^s(\sqrt{1+u^2}) + u^2 \cdot r^p(\sqrt{1+u^2})\right\} \mathrm{d}u \end{aligned} \tag{6}$$

2.1 Angular pattern of dipole emission

By virtue of reciprocity, the local field intensity enhancement factor also represent the probability of emission of a dipole in a particular direction.

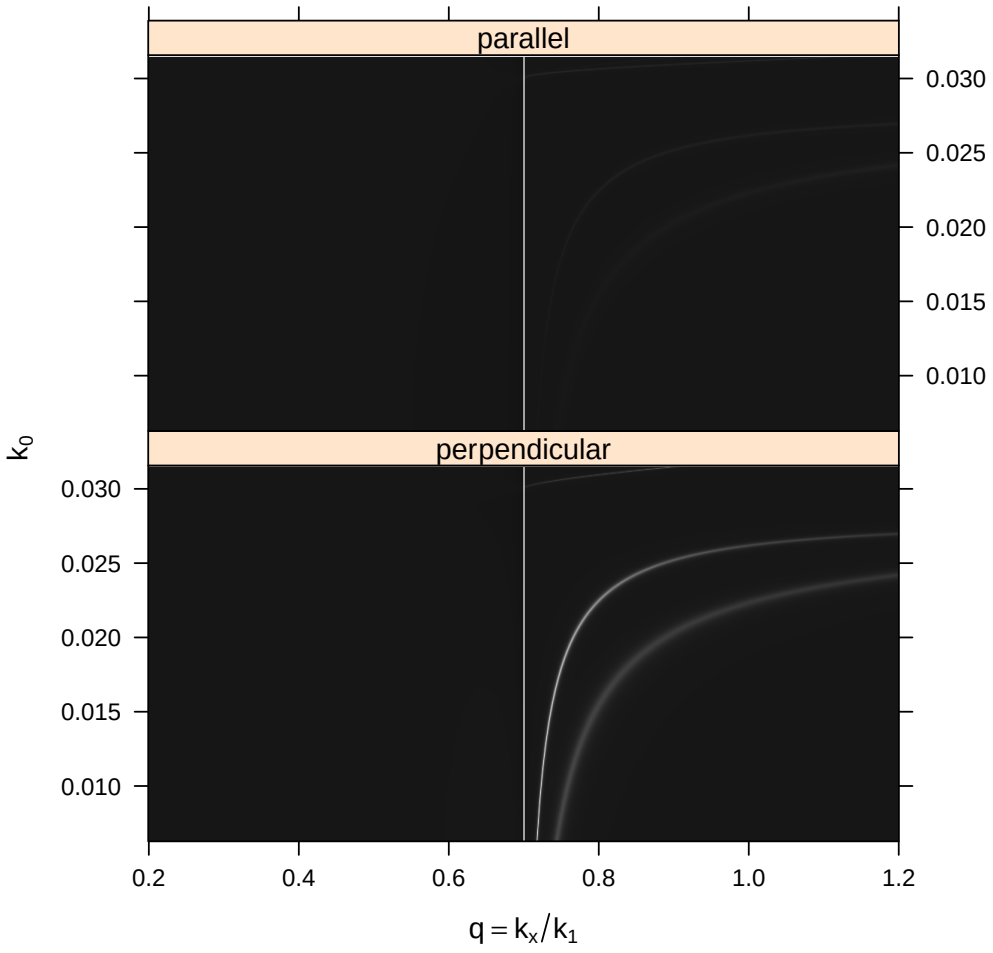

Figure 7: `demo(dipole_integrand)`. Integrand in the resonance region of the total decay rate enhancement factor M_{tot} for a dipole situated 5 nm above a metal interface.

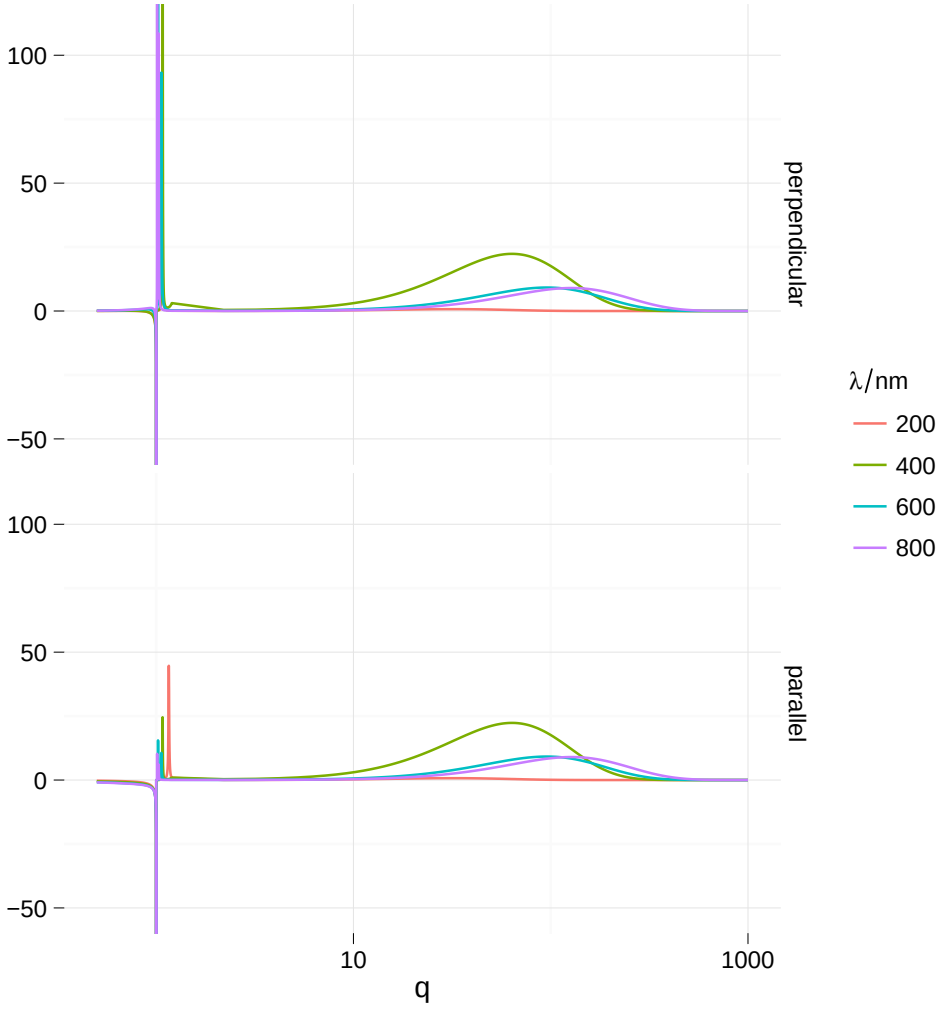

Figure 8: Integrand of the total decay rate enhancement factor M_{tot} for a dipole situated 5 nm above a metal interface, for several emission wavelengths.

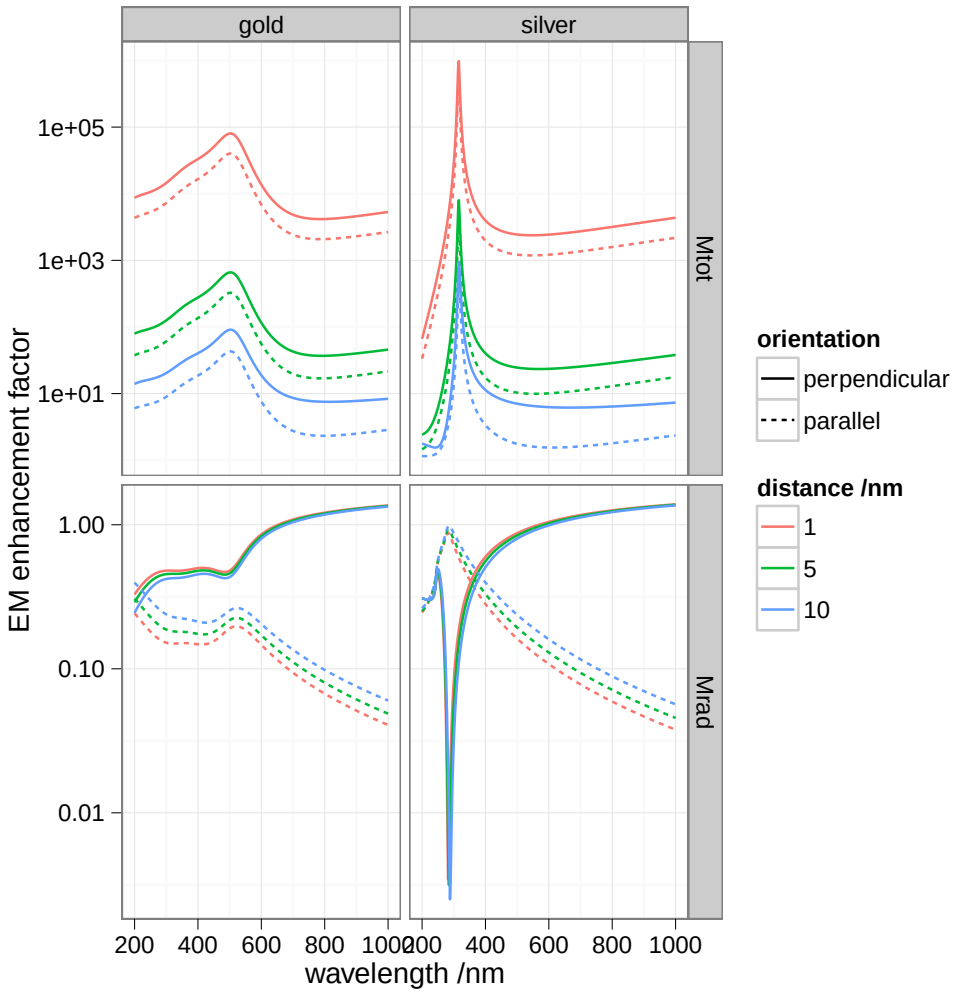

Figure 9: `demo(decay_rates)`. Total and radiative decay rate enhancements for a dipole near a metal interface. Reproducing Fig. 6.1, p. 304 from Principles of Surface-Enhanced Raman Spectroscopy. A dipole is placed near a semi-infinite air/metal interface with orientation either parallel or perpendicular to the interface the total decay rates peak at the wavelength of excitation of planar SPPs epsilon=-1 at the interface (loss channel). The radiative decay rate in the upper medium has a trough at the wavelength where $\varepsilon = 0$ ($Dn = 0$, by continuity $En = 0$).

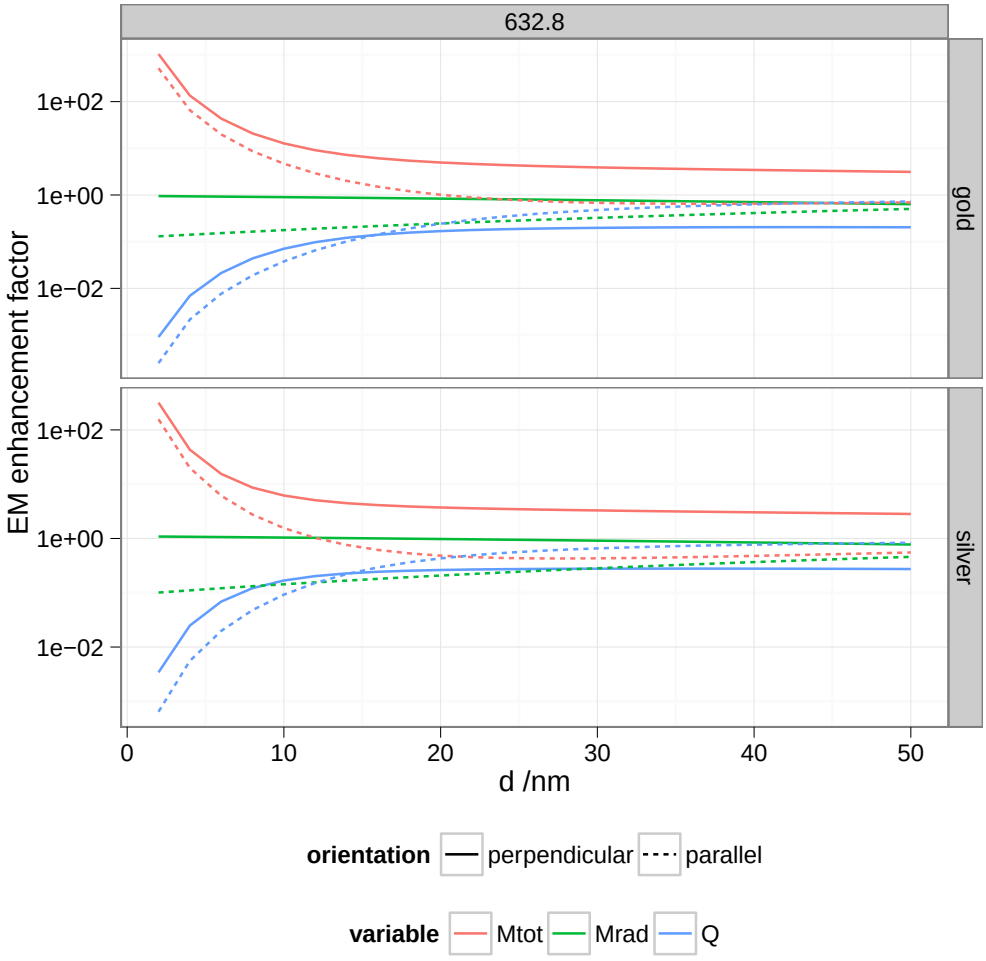

Figure 10: `demo(integrated_decay_rates)`. Integrated decay rates and efficiency for a dipole near a semi-infinite air/metal interface for gold and silver, varying the wavelength and the dipole-interface distance.

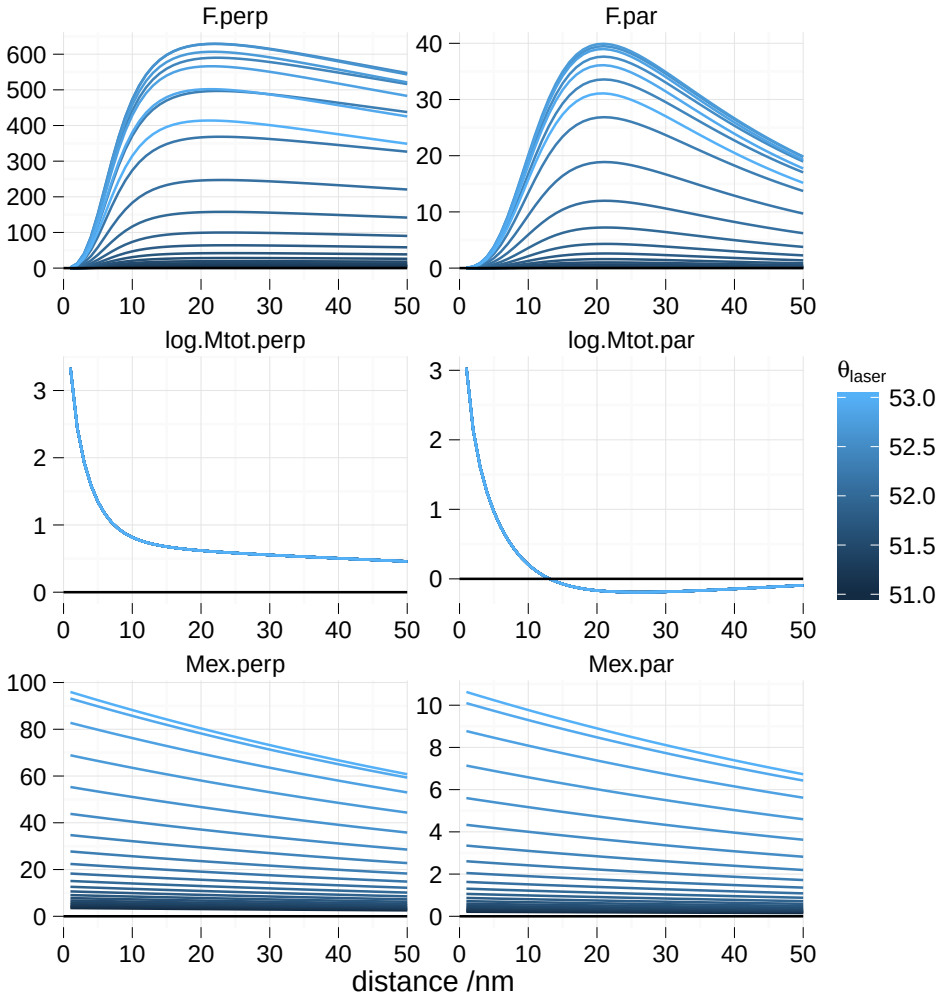

Figure 11: `demo(decay_fluo_distance)`. Fluorescence decay rates vs distance in the Kretschmann configuration.

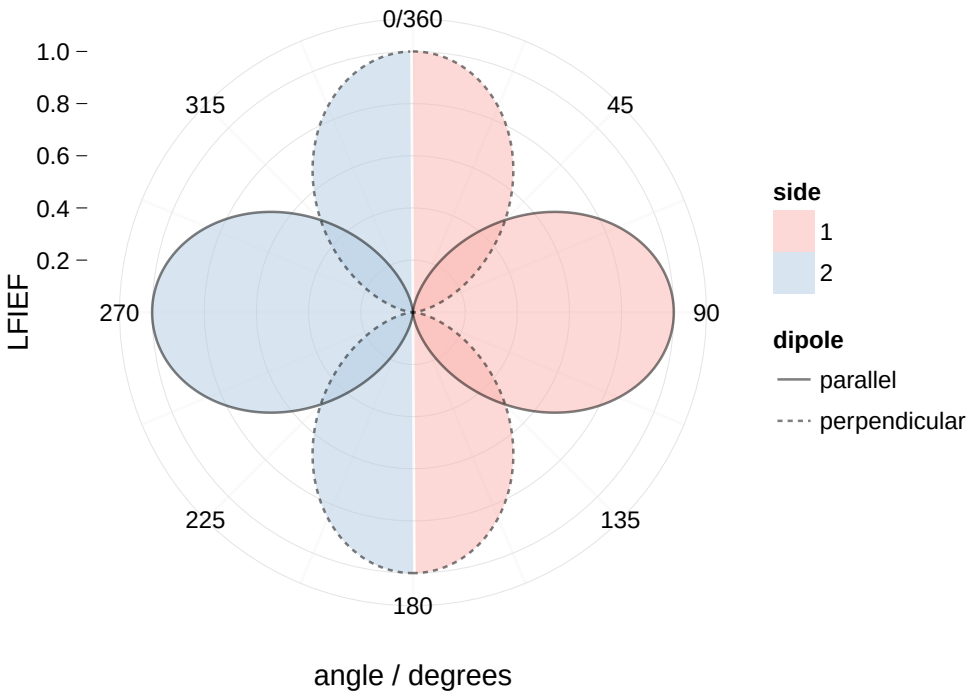

Figure 12: `demo(LFIEF_angular_pattern_dummy)`. Radiation pattern of a dipole in a vacuum (dummy interface, parallel and perpendicular orientation, p-polarisation).

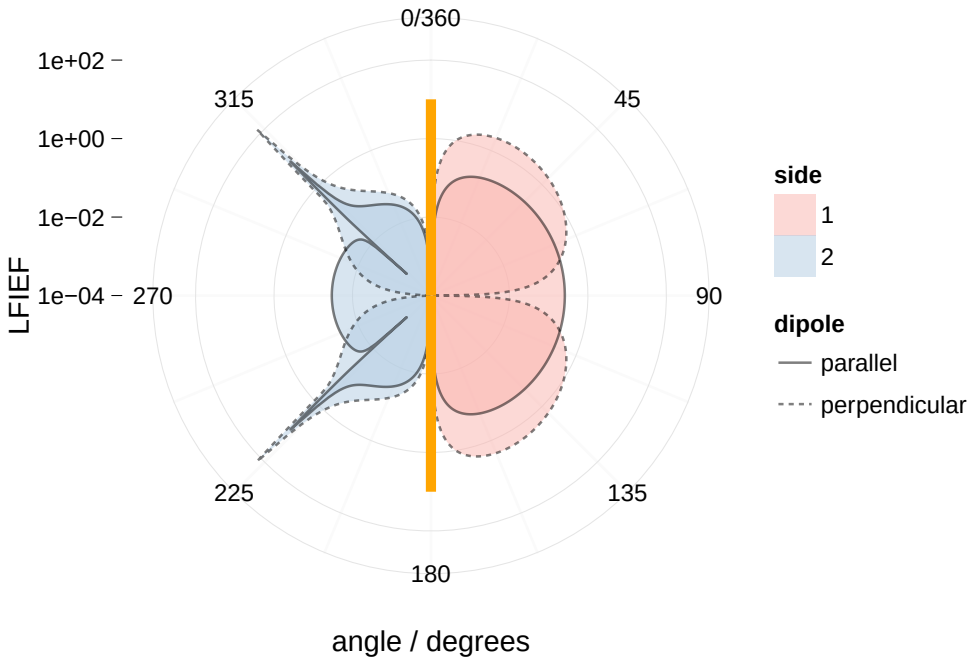

Figure 13: `demo(LFIEF_angular_pattern_kretschmann)`. Radiation pattern of a dipole near a dielectric / metal/ dielectric multilayer, p-polarisation.